AFRL-AFOSR-VA-TR-2018-0408

Synthesis, Characterizaion and Simulation of Ionic Liquids

Mark Gordon
IOWA STATE UNIVERSITY

10/16/2018
Final Report

Air Force Research Laboratory
AF Office Of Scientific Research (AFOSR)/ RTB2
Arlington, Virginia 22203
Air Force Materiel Command

REPORT DOCUMENTATION PAGE

Form Approved
OMB No. 0704-0188

1. REPORT DATE *(DD-MM-YYYY)*	2. REPORT TYPE	3. DATES COVERED *(From - To)*
06-10-2018	Final	From 01-09-2014 to 31-08-2018

4. TITLE AND SUBTITLE

Synthesis, Characterizaion and Simulation of Ionic Liquids

5a. CONTRACT NUMBER

5b. GRANT NUMBER

FA9550-14-1-0306

5c. PROGRAM ELEMENT NUMBER

6. AUTHOR(S)

Mark S. Gordon
Ed Maginn
Robin Rogers

5d. PROJECT NUMBER

5e. TASK NUMBER

5f. WORK UNIT NUMBER

7. PERFORMING ORGANIZATION NAME(S) AND ADDRESS(ES)

Iowa State University, Ames, IA
University of Notre Dame, South Bend, IN
University of Alabama, Tuscaloosa, AL

8. PERFORMING ORGANIZATION REPORT NUMBER

9. SPONSORING/MONITORING AGENCY NAME(S) AND ADDRESS(ES)

Air Force Office of Scientific Research, Arlington, VA

10. SPONSOR/MONITOR'S ACRONYM(S)

AFOSR

11. SPONSOR/MONITOR'S REPORT NUMBER(S)

12. DISTRIBUTION/AVAILABILITY STATEMENT

Public availability

13. SUPPLEMENTARY NOTES

14. ABSTRACT

The overall objective of this project was to carry out synthesis, characterization and theoretical predictions of the properties of energetic ionic liquids. The Gordon group focused on electronic structure calculations on ionic liquid clusters, including investigations of both anions and cations, and on the development of fragmentation methodologies that will enable ab initio molecular dynamics simulations at long enough time scales to be useful for the development of improved classical force fields. The Maginn group focused on three major activities: 1) the development of improved classical force fields for

15. SUBJECT TERMS

Ionic liquids, molecular dynamics, Monte Carlo simulations, ab initio calculations, synthesis, boron additives, activation energies

16. SECURITY CLASSIFICATION OF:			17. LIMITATION OF ABSTRACT	18. NUMBER OF PAGES	19a. NAME OF RESPONSIBLE PERSON
a. REPORT	b. ABSTRACT	c. THIS PAGE			Mark S. Gordon
U	U	U	None	24	19b. TELEPHONE NUMBER *(Include area code)* 515-294-0452

INSTRUCTIONS FOR COMPLETING SF 298

1. REPORT DATE. Full publication date, including day, month, if available. Must cite at least the year and be Year 2000 compliant, e.g. 30-06-1998; xx-06-1998; xx-xx-1998.

2. REPORT TYPE. State the type of report, such as final, technical, interim, memorandum, master's thesis, progress, quarterly, research, special, group study, etc.

3. DATE COVERED. Indicate the time during which the work was performed and the report was written, e.g., Jun 1997 - Jun 1998; 1-10 Jun 1996; May - Nov 1998; Nov 1998.

4. TITLE. Enter title and subtitle with volume number and part number, if applicable. On classified documents, enter the title classification in parentheses.

5a. CONTRACT NUMBER. Enter all contract numbers as they appear in the report, e.g. F33315-86-C-5169.

5b. GRANT NUMBER. Enter all grant numbers as they appear in the report. e.g. AFOSR-82-1234.

5c. PROGRAM ELEMENT NUMBER. Enter all program element numbers as they appear in the report, e.g. 61101A.

5e. TASK NUMBER. Enter all task numbers as they appear in the report, e.g. 05; RF0330201; T4112.

5f. WORK UNIT NUMBER. Enter all work unit numbers as they appear in the report, e.g. 001; AFAPL30480105.

6. AUTHOR(S). Enter name(s) of person(s) responsible for writing the report, performing the research, or credited with the content of the report. The form of entry is the last name, first name, middle initial, and additional qualifiers separated by commas, e.g. Smith, Richard, J, Jr.

7. PERFORMING ORGANIZATION NAME(S) AND ADDRESS(ES). Self-explanatory.

8. PERFORMING ORGANIZATION REPORT NUMBER. Enter all unique alphanumeric report numbers assigned by the performing organization, e.g. BRL-1234; AFWL-TR-85-4017-Vol-21-PT-2.

9. SPONSORING/MONITORING AGENCY NAME(S) AND ADDRESS(ES). Enter the name and address of the organization(s) financially responsible for and monitoring the work.

10. SPONSOR/MONITOR'S ACRONYM(S). Enter, if available, e.g. BRL, ARDEC, NADC.

11. SPONSOR/MONITOR'S REPORT NUMBER(S). Enter report number as assigned by the sponsoring/ monitoring agency, if available, e.g. BRL-TR-829; -215.

12. DISTRIBUTION/AVAILABILITY STATEMENT. Use agency-mandated availability statements to indicate the public availability or distribution limitations of the report. If additional limitations/ restrictions or special markings are indicated, follow agency authorization procedures, e.g. RD/FRD, PROPIN, ITAR, etc. Include copyright information.

13. SUPPLEMENTARY NOTES. Enter information not included elsewhere such as: prepared in cooperation with; translation of; report supersedes; old edition number, etc.

14. ABSTRACT. A brief (approximately 200 words) factual summary of the most significant information.

15. SUBJECT TERMS. Key words or phrases identifying major concepts in the report.

16. SECURITY CLASSIFICATION. Enter security classification in accordance with security classification regulations, e.g. U, C, S, etc. If this form contains classified information, stamp classification level on the top and bottom of this page.

17. LIMITATION OF ABSTRACT. This block must be completed to assign a distribution limitation to the abstract. Enter UU (Unclassified Unlimited) or SAR (Same as Report). An entry in this block is necessary if the abstract is to be limited.

Final Report
AFOSR FA9550-14-1-0306

The PI on this grant was Mark S. Gordon, Iowa State University. The two co-PIs were Ed Maginn (university of Notre Dame) and Robin Rogers (University of Alabama and McGill University). The report is a composite of their efforts. In the following, it is reasonable for the reader to assume that discussions of classical molecular dynamics simulations and reactive Monte Carlo simulations are largely from the Maginn group, discussions of electronic structure theory are largely from the Gordon group, and discussions of experiments are largely from the Rogers group.

1. Objectives

The overall objective of this project was to carry out synthesis, characterization and theoretical predictions of the properties of energetic ionic liquids. The Gordon group focused on electronic structure calculations on ionic liquid clusters, including investigations of both anions and cations, and on the development of fragmentation methodologies that will enable *ab initio* molecular dynamics simulations at long enough time scales to be useful for the development of improved classical force fields. The Maginn group focused on three major activities: 1) the development of improved classical force fields for simulating the bulk properties of ionic liquids; 2) simulations of ionic liquids and their mixtures with molecular compounds; 3) development and application of new simulation methods that can account for chemical reactivity in the condensed phase. The Rogers group focused on synthesis and characterization of ionic liquids.

2. Status of Effort

Developing force fields for energetic ionic liquids

We started by developing force fields for phosphonium cations and reactive cyanopyrrolide and triazolide anions, using energetics obtained from gas phase quantum calculations. Specifically, the cations were triethyloctylphosphonium (P2228) and trihexyltetradecylphosphonium (P66614), while the anions were 2-cyanopyrrolide (2CNpyr) and 4-triazolide (4Triaz). We also developed a force field for the anions reacted with CO_2. Figure 1 shows the structures and names. These ionic liquids were chosen because they would be the test cases used in our simulations of chemical reactivity.

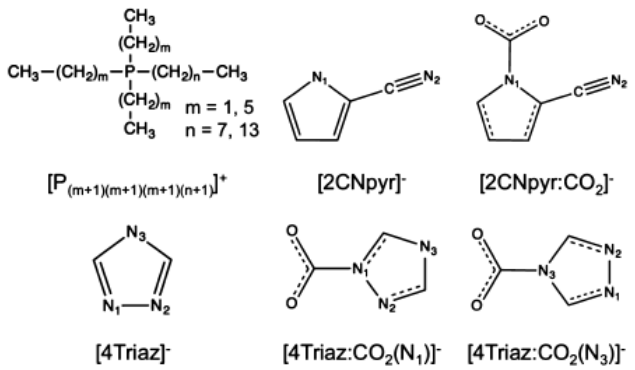

***Figure 1**. Structures of the ions for which force fields were developed. The phosphonium cations have different alkyl chain lengths where m and n are equal to 1 and 7 or 5 and 13 for (P2228) and (P66614), respectively.*

We elected to use a coarse-grained "united-atom" force field in which hydrogen atoms are implicitly represented with the carbon atoms to which they are bonded. For example, simulations modeling a P2228/cnp ion pair with 22 pseudoatoms is more computationally efficient than an all-atom model with 57 atoms. Parameters for the nonbonded van der Waals interactions were taken from the Transferable Potentials for Phase Equilibria (TraPPE) model, a collection of organic molecule force field parameters fit to experimental phase equilibria data. Electrostatic interactions were modeled using fixed partial charges derived by matching the electrostatic potential surface obtained from quantum calculations of an isolated ion. Intramolecular parameters that model angle bending, dihedral rotations and improper bending modes were fit to quantum calculations in which these degrees of freedom were distorted and energy differences computed (see Fig. 2). Using the same procedure, we developed a force field for a larger cation

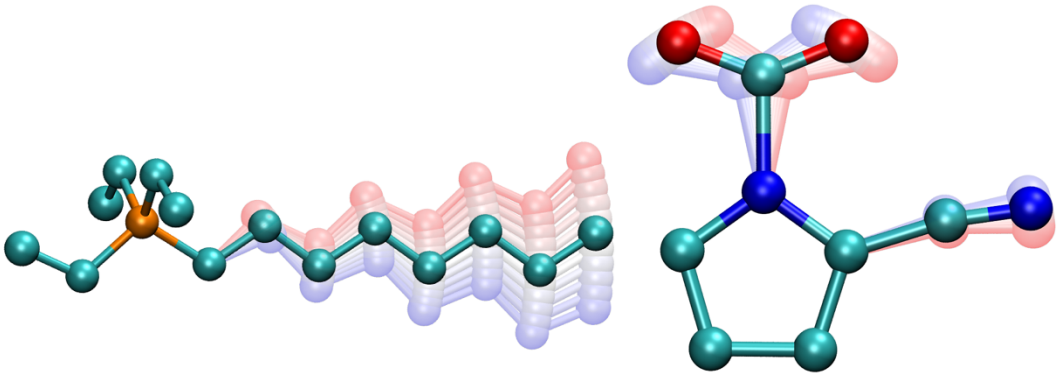

Figure 2. (left) The P-CH2-CH2 angle in P2228 was stretched (blue) and compressed (red). The ab initio energy of each configuration was computed and a harmonic model was fit to the data. (right) The C-N-C angle in cnp-CO_2 was stretched (blue) and compressed (red), inducing a change in the C-C-N angle. A harmonic model was fit to the *ab initio* energy of each configuration.

We tested the accuracy of the force field by simulating neat [P2228][cnp], [P66614][cnp] as well as these ionic liquids once they had reacted with CO_2. Liquid structures in the form of structure functions were computed and compared with experimental results obtained from x-ray scattering experiments. As shown in Fig. 3, the agreement was excellent.

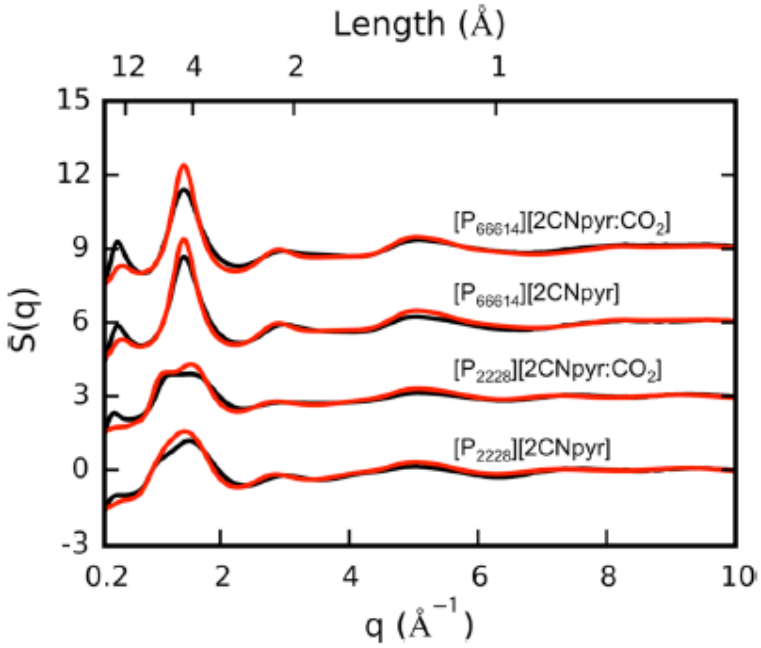

Figure 3. Comparison of experimental and simulated structure functions for all [2CNpyr]− ILs. Experimental structure functions are shown in black. Simulated structure functions are shown in red.
The structure functions are offset by 0, 3, 6, and 9 for [P2228]- [2CNpyr], [P2228][2CNpyr:CO2], [P66614][2CNpyr], and [P66614]- [2CNpyr:CO2], respectively. The primary abscissa (bottom) is in reciprocal space while the secondary abscissa (top) shows the corresponding real space distance.

Force Matching for Potentials

We then moved on to develop more sophisticated (and potentially more automated) ways of generating force fields using force matching procedures. The method is based on an approach first reported by Ercolessi and Adams[1] in 1994. Reference forces between atomic sites *i* and *l* are computed from ab initio simulations performed by the Gordon group and force field parameters are developed in order to minimize the following objective function

$$\chi^2 = \frac{1}{3LN} \sum_{l=1}^{L} \sum_{i=1}^{N} |\mathbf{F}_{il}^{\text{ref}} - \mathbf{F}_{il}^{p}(g_1,\ldots,g_M)|^2$$

where L and N are the number of atoms for sites i and l. The force field forces are F_p with M parameters ($g_1 \ldots g_M$). Note that if L and N are subsets of the total number of atoms in the system, then the integration over neglected degrees of freedom results in a potential of mean force or free

energy between the reduced set of atomic sites. This approach has been used to develop coarse-grained force fields which are thus temperature dependent. In our case, we do not integrate over degrees of freedom but we match the forces F_p for each atom in the system. This gives us a true potential energy (not potential of mean force), such that the derived force field is independent of temperature. Below we show that force fields derived in this way are in fact independent of temperature.

We developed algorithms and software to perform the force matching procedure and tested it on trajectories generated from a classical simulation of water. A box containing 3000 water molecules modeled with the SPC/fw force field was built up and a 20 ns trajectory was generated in the canonical ensemble. 20,000 configurations were saved together with the forces on each atom. To simplify the force matching force field development procedure, only the van der Waals (vdW) interactions were derived using the force matching procedure with all the other parameters (all the bonded parameters as well as partial atomic charges) kept the same as the SPC/fw model. Because SPC/fw water has only one vdW site on the oxygen atom, the development of the force field involves the fitting of the two Lennard-Jones parameters, which are analytically known. The fitting results are shown in Figure 4 (blue line) along with the exact result (red circles). It can be seen from the figure that the force matched parameters agree with the SPC/fw parameters perfectly.

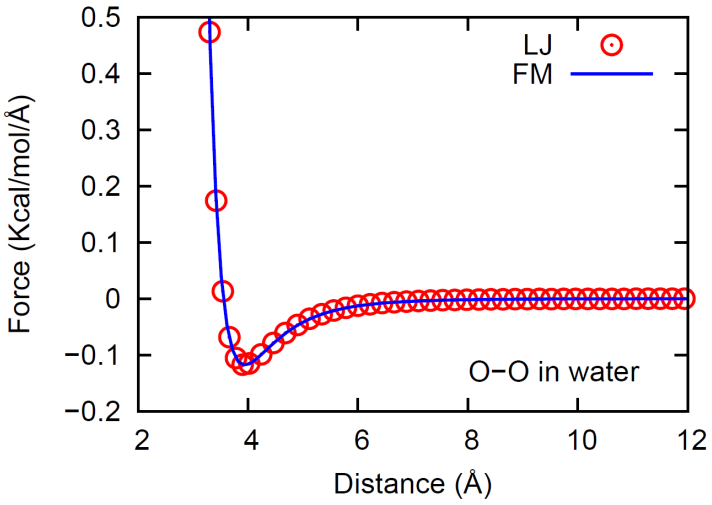

Figure 4: Force matching results for SPC/fw water at 298 K. Force matching was carried out based on 20,000 configurations from 20 ns NVT ensemble simulations. The simulation box had 3,000 water molecules.

Figure 5 shows that there is no temperature dependence of the force field, indicating that this procedure does in fact generate the potential energy and not the free energy.

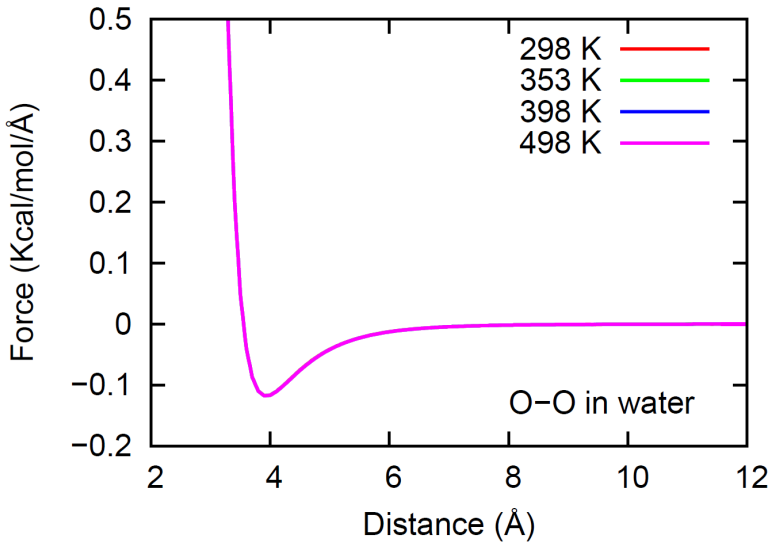

Figure. 5: Force matching result for O-O interactions in water at temperatures ranging from 298K to 498K. All the curves completely overlap so only the 498K is visible.

The same procedure was then applied to the [C1Ntriz][DCA] energetic ionic liquid system. A box a 500 ion pairs was initialized and equilibrated. The interactions were described using the general Amber force field (GAFF) with the partial atomic charges derived using the RESP method based on the electrostatic potential surface calculated for the geometry optimized individual ion at the B3LYP/6-311++g(d,p) level. Similar to the case of water, a trajectory of 20 ns was generated at 350 K in the NVT ensemble and 20,000 configurations were saved for force matching. In this system, there are 11 different atom types and therefore 66 independent pairwise potential functions to derive, which is much more complicated than the water system. Four of the 66 pair potentials are shown in Figure 6. No constraint on the functional form was applied during the force matching process. Therefore, as shown in the plot, the force matched potentials do not necessarily retain the LJ form. Figure 7 shows the structure of [C1Ntriz][DCA].

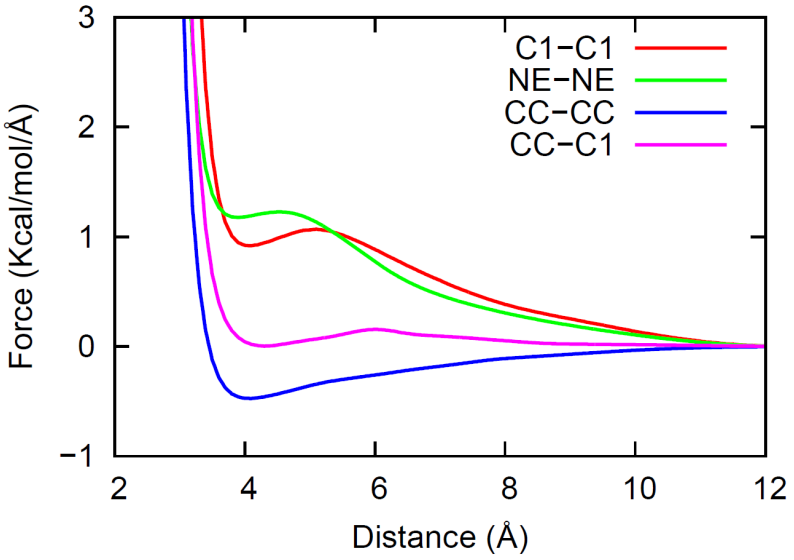

Figure 6: Force matching results for [C1Ntriz][dicyanimide] at 350 K. Force matching was carried out based on 20,000 configurations from 20 ns canonical ensemble simulations. The simulation box had 500 ion pairs. There are 11 atom types in this IL and 66 independent pairwise potentials; four representative functions are shown here between atom types.

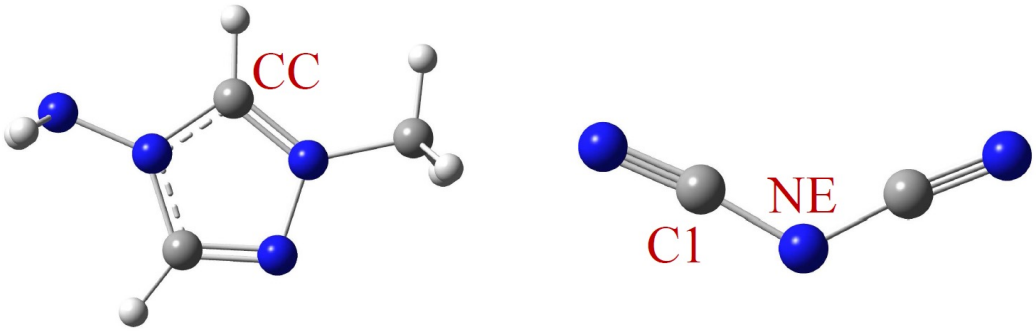

Figure 7: Optimized cation ([C1Ntriz]) and anion ([dicyanimide]) structures in the vacuum at the B3LYP/6-311++g(d,p) level.

Having verified our methods, we performed force matching calculations on ab initio trajectories generated by the Gordon group. We started with a simple system but yet one that is very challenging to get "right" – liquid argon. This is a difficult test of force matching because the dispersion interactions between argon are weak. The calculations were performed by first carrying out a classical simulation of the bulk liquid. From this, 741 independent "snapshots" were taken from the trajectory and for each one of these, a small droplet of argon was removed containing about 100 atoms. The forces were then calculated quantum mechanically and the force matching procedure was used. Figure 8 shows the result compared to an accurate Lennard-Jones (LJ) potential.

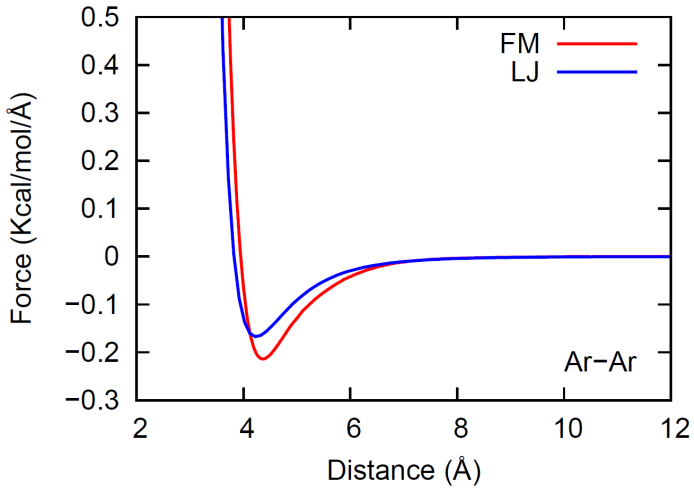

Figure 8: Force matched (FM) and accurate forces from the accepted Lennard-Jones potential (LJ) of argon.

The force matched potential is very similar to the Lennard-Jones potential, although the location of the position of the minimum is about 0.02 nm larger than the LJ potential and the FM result is slightly more attractive that the LJ potential. We fit the force matched potential to a new LJ potential and then used it in classical simulations to test its predictive capability.

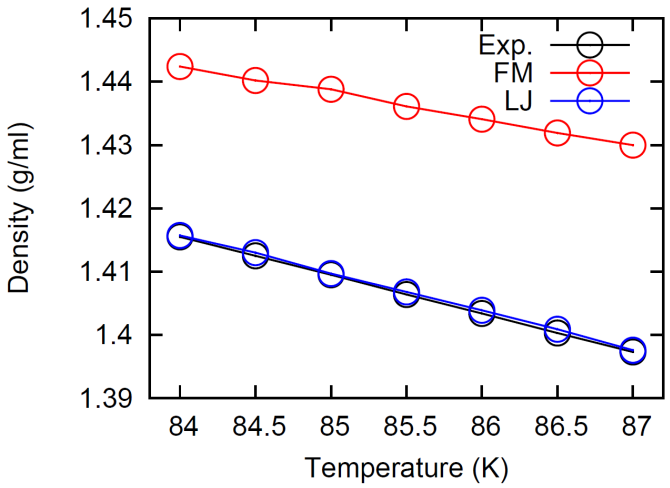

Figure 9: Computed liquid density as a function of temperature for the FM and empirical LJ potential. The LJ potential is in quantitative agreement with experiment, while the FM potential gives densities that are slightly higher than experiment.

As can be seen in Fig. 9, the FM potential gives densities that are 1-2% higher than experiment, while the empirical LJ potential gives nearly perfect agreement (which is not surprising, since it was fit to experimental data).

Fig. 10 shows the computed radial distribution functions (RDFs) for NaCl at 85 K using the FM and LJ potential. The structures are quite similar and agree well with experimental data.

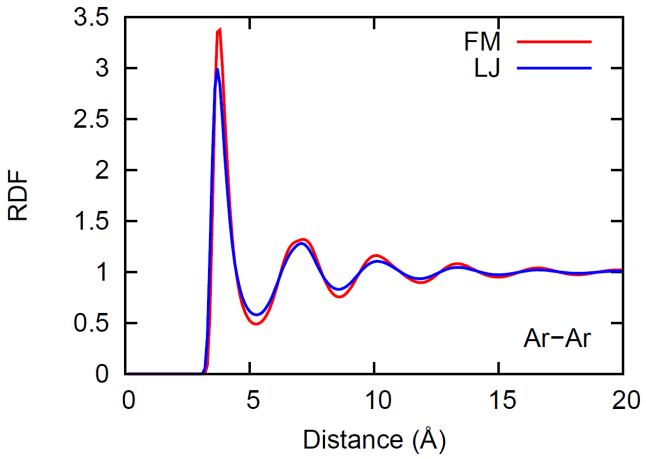

Figure 10: Radial distribution function (RDF) for argon at 85K obtained with LJ and FM potentials.

We also computed vapor-liquid coexistence curves for argon as well as vapor pressures using the FM and LJ potentials. Fig. 11 shows a comparison with experimental data. As expected, the more attractive FM potential has a higher critical temperature and lower vapor pressure than the LJ potential or experiment. These results show how sensitive these properties are to small differences in potential energy.

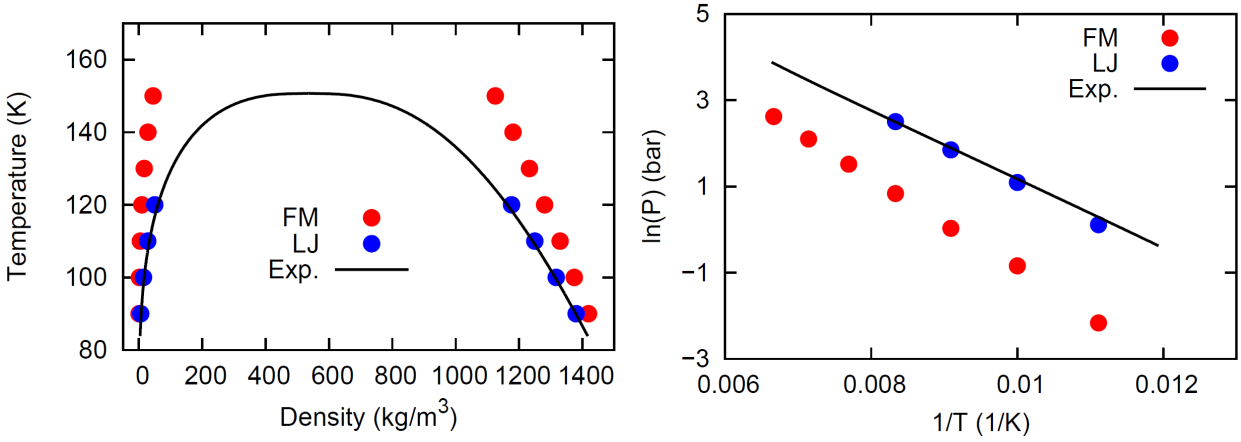

Figure 11: (left) Vapor-liquid coexistence curve and vapor pressure (right) for argon.

The melting point of argon was computed and found to be 103.7 K for the FM model and 82.8 K for the LJ model. The experimental value is 83.81 K, showing that the FM model overestimates

the melting temperature. Finally, we computed the enthalpy of vaporization as a function of temperature. Figure 12 shows the results. Again, the FM potential overestimates the enthalpy due to it being slightly too attractive, but differs from experiment by less than 3 kJ/mol. The net result of this work is that the FM approach does a reasonable job estimating a potential although empirical potentials fit to experimental data can be more accurate.

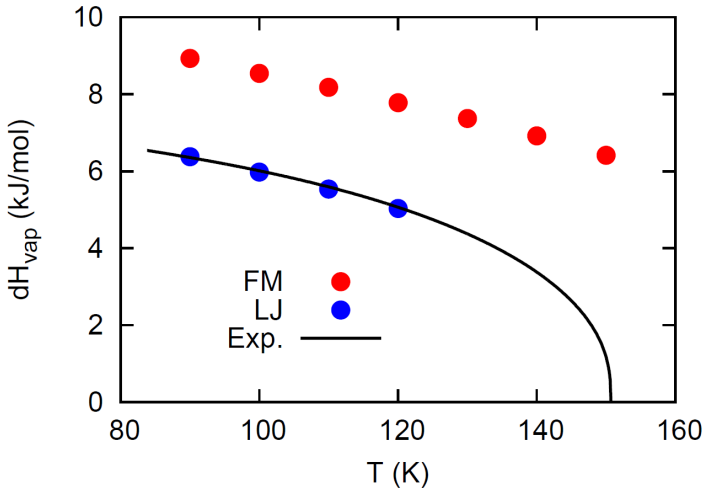

Figure 12: Computed enthalpy of vaporization for argon as a function of temperature for the FM and LJ potentials compared to experiment.

We are in the process of applying this method to water and energetic ionic liquids. We have found that the strong intramolecular interactions present in these systems leads to difficulties in getting reasonable forces. In addition, the ab initio calculations are very challenging and time consuming. We had not successfully developed a FM potential for these more complex molecules by the end of the project but are continuing to make progress.

Reactive Monte Carlo simulations

We have developed a reactive Monte Carlo (RxMC) method that can be used to study how solvation and confinement change the equilibrium distribution of products in reactive systems. As reported previously, we used this RxMC method to compute reactive absorption isotherms of CO_2 in the ionic liquid triethyl-octylphosphonium 2-cyanopyrrolide ([P2228][2CNpyr]). Figure 13 shows the comparison of computed and experimental results.

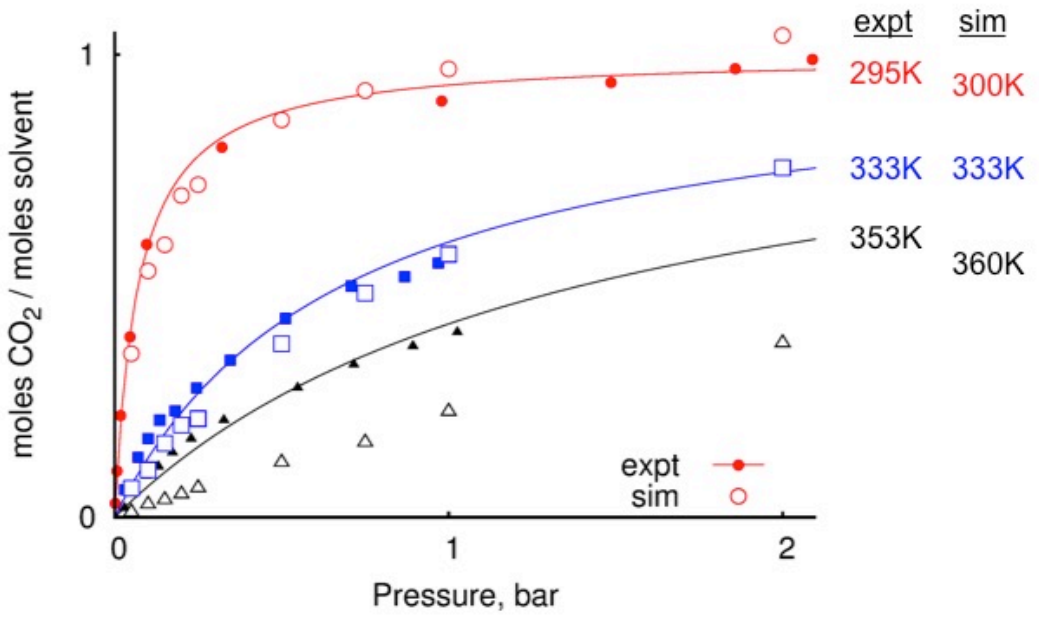

Figure 13: Experimental (filled symbols) and computed (open symbols) isotherms for CO_2 in the reactive ionic liquids [P2228][2CNpyr].

We have also applied the RxMC method to study reactions in the condensed phase. As a simple test system, we examined the isomerization of xylene in the liquid phase and under confinement in carbon nanotubes. Figure 14 shows that the liquid phase product distribution is captured quantitatively by the RxMC simulations.

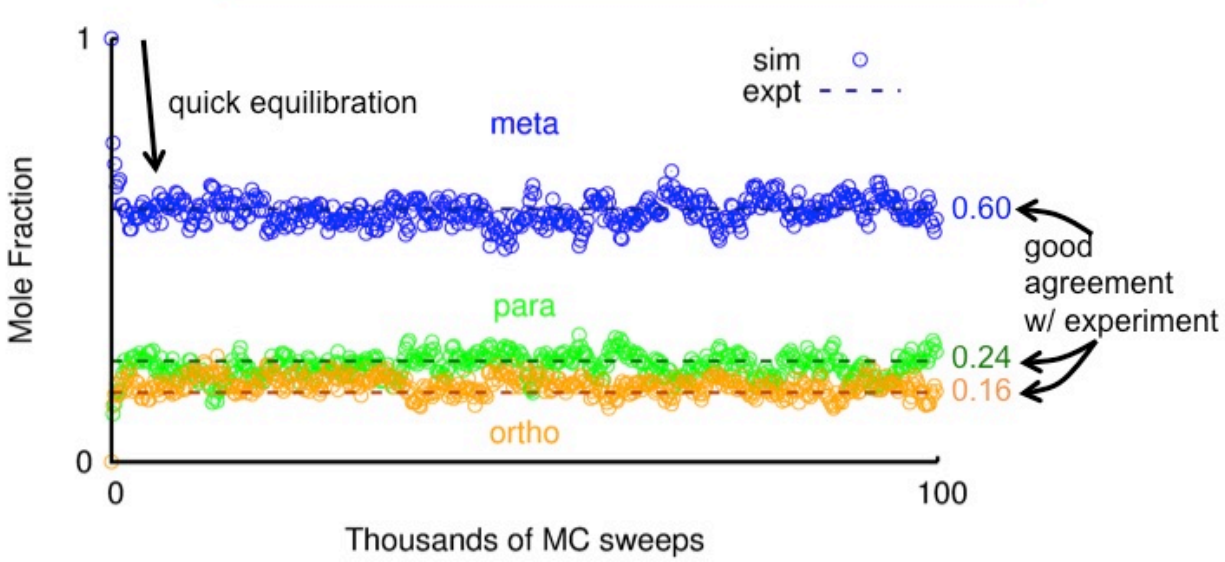

Figure 14: RxMC simulations of xylene isomerization reaction product distribution in the liquid phase. The simulations agree quantitatively with experiment.

We then applied the RxMC method to a confined system. It is known that zeolite catalysts can shift the equilibrium product distribution of xylene toward the more valuable p-xylene isomer, and it is thought that this is caused by confinement effects that either shift the equilibrium product distribution toward the "smaller" p-xylene isomer or diffusion limitations that only allow the p-xylene isomer to escape from the pores of the zeolite. To test this hypothesis, we simulated the xylene isomerization process in a series of carbon nanotubes with varying pore diameters. Figure 15 shows the results.

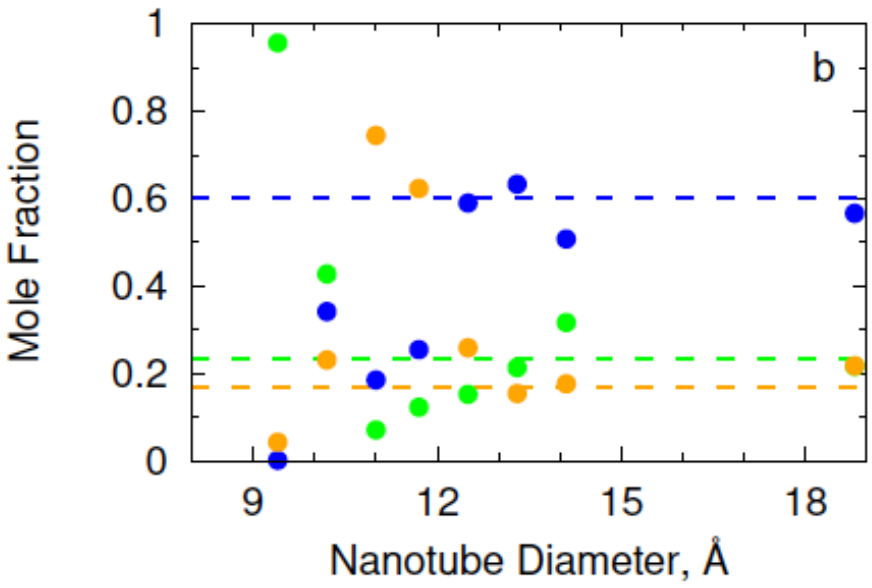

Figure 15: Computed mole fractions of m-xylene (blue), p-xylene (green) and o-xylene (orange) as a function of nanotube pore diameter. Dashed lines show the equilibrium composition for the liquid phase.

The results show that large pore nanotubes (1.8 nm or so) have no effect, yielding product distributions virtually identical to the liquid phase. The very smallest diameter pores yield almost 100% p-xylene, consistent with experimental results found in zeolites. Unexpectedly, we find that pores of intermediate size favor o-xylene, and that this is caused by the fact that of the three isomers, x-xylene retains the greatest rotational entropy inside pores of intermediate diameter. The results suggest that RxMC can be used to study how confinement effects in zeolites, metal organic framework materials and other nanoporous catalysts can be used to shift product distributions toward desired products.

In future studies, we plan to apply RxMC to study how reaction pathways of intermediates are altered because of solvation effects. For example, it is known that the solvation environment changes the relative free energies of different intermediates during the hypergolic combustion of energetic ionic liquids. These solvation effects are currently treated in an approximate "continuum" manner in quantum chemical studies. The RxMC approach can be coupled with high level gas phase quantum calculations to more accurately determine free energies of reactive intermediates and thus can help elucidate combustion pathways.

Evaluation of Classical Force Fields for Water-Ionic Liquid Systems

As a test of the ability of standard classical force fields to capture the properties of important systems, we undertook a systematic study of water solubility in three imidazolium-based ILs with different degrees of hydrophobicity: 1-n-butyl-3-methylimidazolium hexauorophosphate ([C4mim][PF6]), 1-n- butyl-3-methylimidazolium bis(triuoromethylsulfonyl)imide ([C4mim][Tf2N]) and 1-n-butyl-3-methylimidazolium chloride ([C4mim][Cl]). An evaluation of

several water models and various IL force fields was conducted. The selected water models are the TIP5P, TIP4P2005 and a collection of three site models based on the SPC geometry but with different sets of fixed partial charges. These partial charges are consistent with water surrounded by different electrostatic environments, and crudely account for polarizability. In the case of the IL force fields, net partial charges of +/- 1.0e were used. In addition, scaled charges of +/-0.9e and +/-0.8e were used to account for polarization and charge transfer. It is found that most water models tested with the full charge [C4mim][PF6] and [C4mim][Cl] force field overestimate the solubility, but the agreement is reasonably good with [C4mim][Tf2N]. Attempts at improving the results by either scaling the charges on the IL or on water were made, but no combination was able to reproduce experimental phase behavior satisfactorily. The main conclusion of the study is that, to consistently model water absorption in ILs, force fields that include effects such as polarization are likely necessary. It further motivates our work on developing force matched force fields from ab initio simulation. The results of this study appeared in *Fluid Phase Equilibria*, **2016**, 407, 117-125.

Cyano-Based Ionic Liquids and Glucose

Among different classes of, those with cyano-based anions have been of special interest due to their low viscosity and enhanced solvation ability for a large variety of compounds. Experimental results reveal that the solubility of glucose in some of these ionic liquids may be higher than in water – a well-known solvent with enhanced capacity to dissolve mono- and disaccharides. This raises questions on the ability of cyano groups to establish strong hydrogen bonds with carbohydrates and on the optimal number of cyano groups at the IL anion that maximizes the solubility of glucose. This has obvious consequences for the development of environmentally benign solvents for conversion of biomass to fuels. We used a combination of density functional theory (DFT) and molecular dynamics (MD) simulations to examine these systems. Through the calculation of the number of hydrogen bonds, coordination numbers, energies of interaction and radial and spatial distribution functions, it was possible to explain the experimental results and to show that the ability to favorably interact with glucose is driven by the polarity of each IL anion, with the optimal anion being dicyanamide.

Effect of water on Ionic Liquid Stability. Because the presence of water can significantly diminish the efficacy of energetic ionic liquids as fuels, an investigation was initiated into the effects of the presence of water molecules on the propensity for proton transfer from the cation to the anion in an ionic liquid. Previously, we had found that if only one cation-anion pair is present in a calculation, the proton jumps from the cation to the anion with no barrier to form a neutral pair. However, when two cation-anion pairs are present the ionic separation is stable to proton transfers, and the separated ion pairs are lower in energy than the neutral pairs at the coupled cluster level of theory. Water is predicted to behave in much the same way. If one water molecule is added to a cation-anion pair, the water molecule acts as a conduit for the passing of a proton from the cation to the anion. However, when two water molecules are present, the waters orient themselves in such a way as to stabilize the separated ions enough that this arrangement is more stable than the corresponding arrangement in which a double proton transfer has occurred.

That is, the separated ion species is now the global minimum. In fact, nearly all of the minima on the 1,2,4-triazolium dinitramide (TN) system with two waters present are separated ion minima. The barriers separating the neutral pair from the separated ion pair in various conformations are very small (less than 3 kcal/mol), suggesting that the neutral pairs do not even exist. An example is shown in the following figure, in which A' is a neutral pair and A is a separated ion pair. Insight into the neutral vs. separated ion relative energies is enhanced by the use oriented quasi-atomic orbitals (QUAOs) that are also pictured in the figure. This work has recently been published in the Journal of Physical Chemistry A.

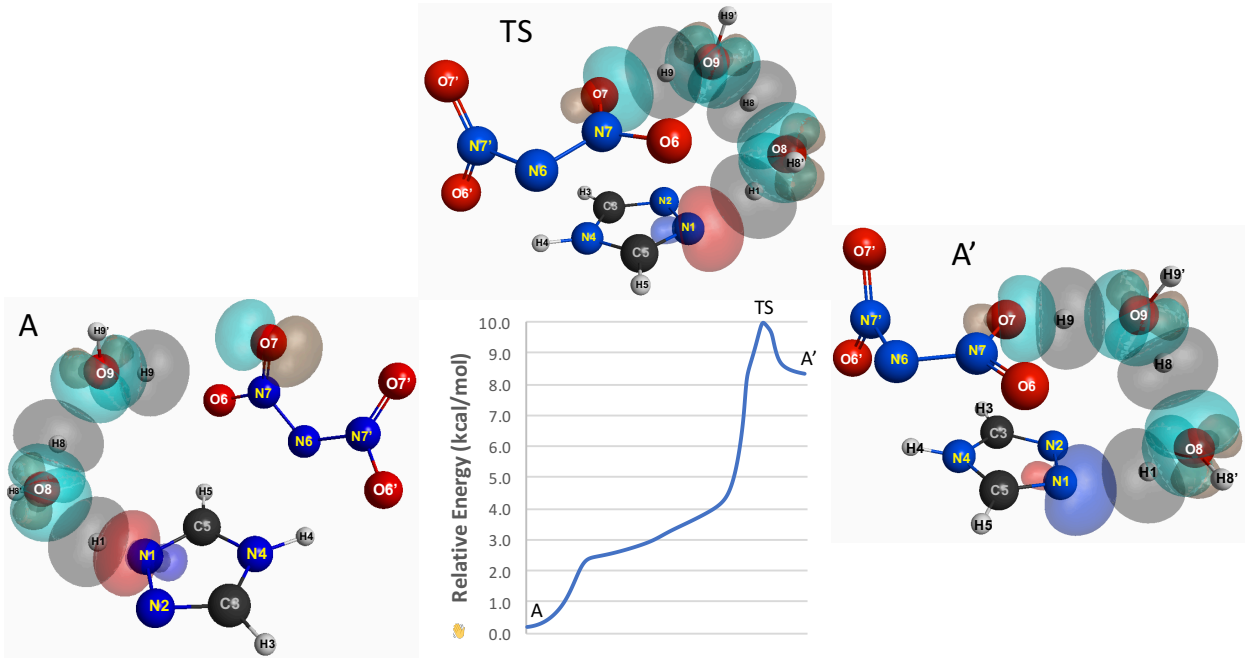

The role of the cation in ionic liquids. The protonation of the anion in an ionic liquid plays a key role in the hypergolic reaction between ionic liquids and oxidizers like white fuming nitric acid. To investigate the influence of the cation on the protonation reaction, the deprotonation energy of a set of cations has been calculated at the MP2 level of theory. Specifically, guanidinium, dimethyltriazanium, triethylamine, N-ethyl-N-methyl-pyrrolidinium, N-ethyl-pyridinium, 1,4-dimethyl-1,2,4-triazolium, 1-ethyl-4-methyl-1,2,4-triazolium, and 1-butyl-4-methyl-1,2,4-triazolium were studied. In addition, the net proton transfer energies from the cations to a set of previously studied anions has been calculated, demonstrating an inverse correlation between the net proton transfer energy and the likelihood that the cation/anion combination will react hypergolically with white fuming nitric acid. It is suggested that this correlation occurs due to a balance between the energy released by the proton transfer and the rate of proton transfer as determined by the ionicity of the ionic liquid. This may be seen in the following table that shows the net MP2 proton transfer energies. The columns in the table are arranged in order of decreasing proton affinity from left to right. The NPT energies also decrease from left to right. The average NPT energy for each anion, determined by averaging the NPT energy of all combinations of the anion with the cations included in this work, is given in the last

row. Of the four anions with the smallest average NPT energy, dicyanamide and dicyanoborohydride have been shown to react hypergolically with WFNA for a wide range of cations. Cyanoborohydride has also been shown to react hypergolically with WFNA for some cations, but is not as thoroughly tested because the ionic liquids are hygroscopic. Of the four anions with the largest average NPT energy, azide, phosphinate, and nitrate form ionic liquids that either do not react hypergolically or exhibit very long ignition delays. This result matches the positive correlation demonstrated for monomolecular fuels by McQuaid that ignition delays increase in direct proportion with the proton affinity, including a lack of ignition for the largest proton affinities

Net energy change of proton transfer reaction in eV

	N_3^-	$PH_2O_2^-$	BH_4^-	NO_3^-	$N(NO_2)_2^-$	$N(CN)_2^-$	BH_3CN^-	ClO_4^-	$BH_2(CN)_2^-$
DMT	-3.42	-3.28	-3.26	-3.04	-2.49	-2.35	-2.18	-2.05	-0.98
TEA	-4.34	-4.20	-4.18	-3.96	-3.41	-3.27	-3.10	-2.97	-1.90
EMPyrr	-2.51	-2.37	-2.34	-2.12	-1.57	-1.44	-1.26	-1.13	-0.06
EPyr	-3.07	-2.93	-2.91	-2.69	-2.14	-2.00	-1.83	-1.70	-0.63
Guan	-4.24	-4.10	-4.08	-3.86	-3.31	-3.17	-3.00	-2.87	-1.80
MMTZ	-3.64	-3.50	-3.48	-3.25	-2.71	-2.57	-2.40	-2.27	-1.19
EMTZ	-3.57	-3.43	-3.41	-3.18	-2.64	-2.50	-2.32	-2.20	-1.12
BMTZ	-3.56	-3.42	-3.40	-3.18	-2.63	-2.49	-2.32	-2.19	-1.12
Average	-3.55	-3.41	-3.38	-3.16	-2.61	-2.47	-2.30	-2.17	-1.10

Effect of boron clusters on hypergolic ignition. Many ionic liquids containing the dicynamide anion (DCA^{-1}, formula $N(CN)_2^{-1}$) exhibit hypergolic ignition when exposed to the common oxidizer nitric acid. However, the ignition delay is often about ten times longer than the desired 5 milliseconds for rocket applications, so that improvements are desired. Experiments in the last decade have suggested both a mechanism for the early reaction steps, and also that additives such as decaborane can reduce the ignition delay. The mechanism for reaction of nitric acid with both DCA^{-1} and protonated DCAH have been considered, using accurate wave function methods. Complexation of DCA^{-1} or DCAH with borane clusters $B_{10}H_{14}$ or $B_9H_{14}^{-1}$ is found to modify these mechanisms slightly, by changing the nature of some of the intermediate saddle points and by small reductions in the reaction barriers. However, according to these calculations, the boron clusters do not have a significant impact on the mechanism or energetics. A paper on this effort has been published.

EFMO gradients. Previously, fully analytic gradients have been derived and implemented for the fragment molecular orbital (FMO) method, and we have shown that fully analytic gradients are essential to obtain adequate energy conservation in molecular dynamics (MD) simulations. The FMO MD method is now being used to conduct simulations on ionic liquids in order to

provide insight into bulk properties. The plan is to extract from these MD simulations sufficient information about the potentials to coarse grain the ab initio potentials onto much simpler and computationally less expensive classical models. This latter effort is in collaboration with the Maginn group. FMO MD simulations will be part of an invited PCCP perspective paper on ionic liquids that will be submitted shortly. In order to provide faster and more accurate MD simulations, the fully analytic gradient for the effective fragment molecular orbital (EFMO) method has now been completed. The EFMO method is an integration of the FMO and effective fragment potential (EFP) methods, in which the simple FMO electrostatic potential is replaced with the EFP potential. When a pair of fragments (a dimer) is far enough apart, their interaction energy is calculated with the EFP method, rather than the chosen *ab initio* method (e.g., second order perturbation theory). This approach saves considerable computer resources (time and memory) relative to the second order FMO method, FMO2, while also providing improved accuracy. A paper that reports the EFMO analytic gradient has been published. A demonstration that the EFMO analytic gradient can be used to perform EFMO MD simulations is included in the paper. The following figure shows a log-log plot of seven EFMO MD simulations of a 32-water cluster in the NVE ensemble using six different time step sizes vs. the RMSD(E) of the energy. The slope of this plot is 2.03, very close to the ideal slope of 2.0.

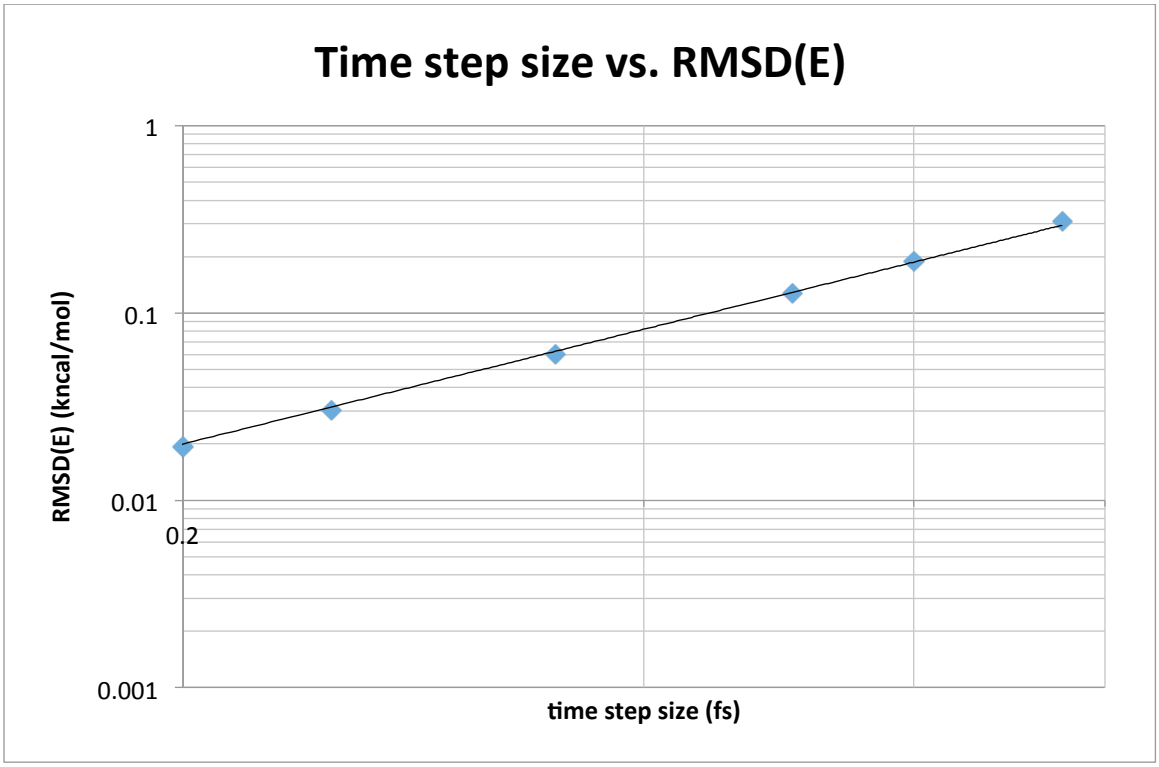

Ab initio Monte Carlo method. The GAMESS MC code has now been generalized so that, in addition to the EFP method, it can be applied to any ab initio method in GAMESS, including the FMO and EFMO methods. This will be very important for the prediction of global minima in ionic liquid and ionic liquid-water clusters.

Ionic liquid experiments. The Rogers group have continued to investigate the combination of *n*-$B_{10}H_{14}$ with energetic organic molecules and salts to increase the energy content of the

resulting species. A large series of novel functionalized borane clusters were isolated and characterized, representing several new strategies for using these compounds. In many cases, the compounds showed remarkable hypergolicity in typical drop tests using white fuming nitric acid (WFNA) as an oxidizer.

Building on the observation that ionic liquids (ILs) can react with *n*-$B_{10}H_{14}$ to make hypergolic species (see Rogers *et al.*, *Inorg. Chem.* **2014**, *53*, 4770 and *ChemPlusChem* **2016**, *81*, 922), we have continued to explore the functionalization of *n*-$B_{10}H_{14}$ with the azoles used to make energetic ILs. An overview of the most relevant synthetic pathways is summarized in **Scheme 1**. These strategies include covalent modification of *n*-$B_{10}H_{14}$ with functionalized imidazoles and with linker groups which can bridge multiple clusters to enhance their hypergolic response. We have also explored whether the grafted moieties can interact noncovalently with energetic guests to make new multicomponent solids.

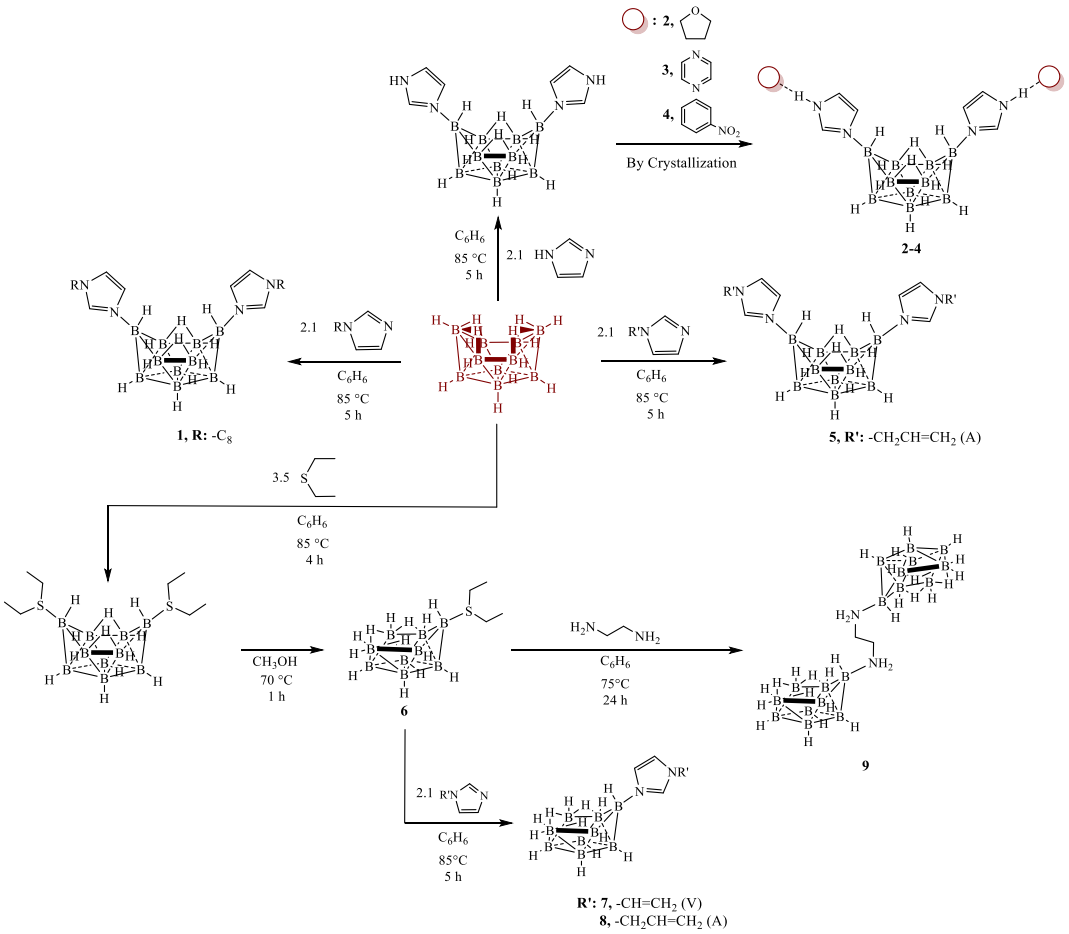

Scheme 1. Syntheses of **1-9**

The symmetrical functionalization of *n*-$B_{10}H_{14}$ with 1-alkyl-functionalized imidazole allowed us to test the resulting compounds as additives for flammable molecular solvents (MeOH, EtOH, THF, EtOAc, and kerosene). About the experiments with kerosene, which is the major fraction of RP-1 and RP-2 fuels, we utilized **1** and the already reported $(Rim)_2B_{10}H_{12}$ (with R: H, C_1, C_2,

C_4) to verify if they could induce hypergolicity both in homogeneous solutions and in mixtures. In the last case, we proved that it is possible to achieve this important goal (**Table 1**).

Table 1. Isolated $(Rim)_2B_{10}H_{12}$ where R: H, C_1, C_2, C_4 and C_8 and IDs in kerosene mixtures

Material/Formula	Crystal Structure	Ignition Delays in kerosene mixtures
$(Him)_2B_{10}H_{12}$ $[C_6H_{20}B_{10}N_4]$	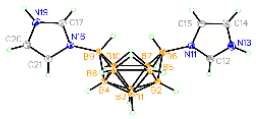	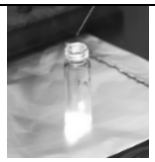 35 ms
$(C_1im)_2B_{10}H_{12}$ $[C_8H_{24}B_{10}N_4]$	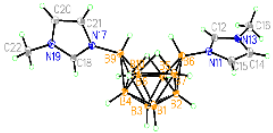	 31 ms
$(C_2im)_2B_{10}H_{12}$ $[C_{10}H_{28}B_{10}N_4]$	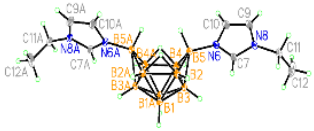	 564 ms
$(C_4im)_2B_{10}H_{12}$ $[C_{14}H_{36}B_{10}N_4]$	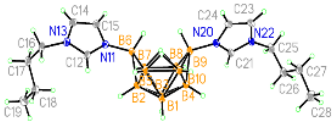	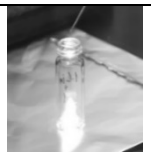 4 ms
1, $(C_8im)_2B_{10}H_{12}$ $[C_{22}H_{52}B_{10}N_4]$	The structure has not been isolated yet.	 4 ms

In additional preparative approaches aiming to bind multiple boron hydride clusters in a single unit, we utilized an accessible precursor $(Et_2S)_2B_{10}H_{12}$ for its partial dismantling to a B_9H_{13}-based cluster, followed by ligand exchange in the presence of 1-olefin-functionalized imidazoles, *i.e.* Vim and Aim, and primary diamines, *i.e.* 1,2-diaminoethane and 1,4-diaminobutane. Additional tests involved 1,4-phenylenediamine can be seen in the same context. As sketched in **Scheme 1**, we could isolate and characterize by single crystal X-ray diffraction, an example of multiple boron hydride clusters entrapped in a single structure by a bidentate molecular linker, *i.e.* 1,2-diaminoethane (**Table 2**). Recently, we started to explore also the 1,4-bis(imidazole)butane for the same purposes. The possibility to graft 1-olefin-functionalized azoles on a B_9H_{13}-based cluster, in combination with the synthesis of **5** and the already mentioned homolog $(Vim)_2B_{10}H_{12}$, offers the initial instruments to explore the preparation of

dimeric and oligomeric compounds by ruthenium-catalyzed olefin metathesis and titanium-catalyzed hydroboration.

Table 2. Crystal Structures and IDs (neat compounds) for the synthesized compounds

Material/Formula	Crystal Structure	Ignition Delays
5, $(Aim)_2B_{10}H_{12}$ $[C_{12}H_{30}B_{10}N_4]$	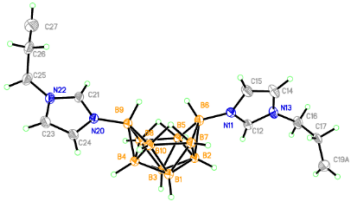	Not Measured
2, $(Vim)B_9H_{13}$ $[C_{10}H_{24}B_{10}N_4]$	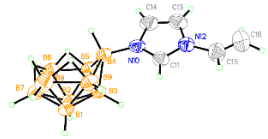	Not Measured
9, $(NH_2CH_2CH_2NH_2)(B_9H_{13})_2$ $[C_{14}H_{46}B_{18}N_2]$	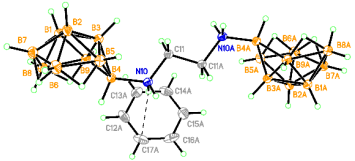	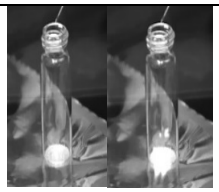 0 ms 1(0) ms
$(o\text{-PDA})B_9H_{13}$[a] $[C_6H_{21}B_9N_2]$	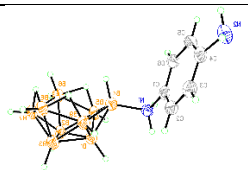	Not Measured
$(pyrazine)_2B_{10}H_{12}$[b] $[C_4H_{16}B_{10}N_2]$	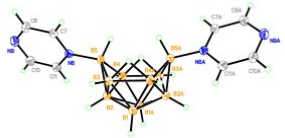	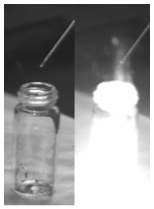 1 ms 7 ms

[a]The compound was isolated in the attempt to make a dimeric structure analog to **9**.

[b]Preliminary results demonstrated that the methodology applied to the imidazole- based compounds could be extended to alternative suitable substrates, *e.g.* the pyrazine.

Encouraged by the mentioned outcomes and based on the physicochemical characteristics of the azole-functionalized decaborane, we aimed to further tailor critical physical characteristics, *i.e.* oxygen balance, density, and heat of formation, and, consequently, to tune the performance of the new energetic materials by forming multicomponent solids. We have started to investigate examples of non-covalent derivatization of the *exo*-6, *exo*-9 imidazole-substituted *nido*-decaborane in the presence of hydrogen donors and acceptors such as solvents (benzene and THF) and

energetic or non-energetic co-former, *e.g.* toluidine, pyrazine and nitrobenzene. The aim is to tailor Up to now, we demonstrated the effect of co-crystallization and hypergolicity of new materials mainly with $(im)_2B_{10}H_{12}$. The crystallization of the compounds was occurred by simple slow evaporation technique using typical organic volatile solvents such as acetone, THF, and benzene. The resulting compounds exhibit impressive performance with low ignition delays and higher densities, especially in the presence of nitrobenzene. Noteworthy, the results with the pyrazine, which is not considered as energetic co-former, highlighted an impressive hypergolic performance (**Table 3**).

Table 3. Crystal Structures and IDs (neat compounds) for the synthesized cocrystals

Material	Crystal Structure	Ignition Delays
2, $(Him)_2B_{10}H_{12}$·THF	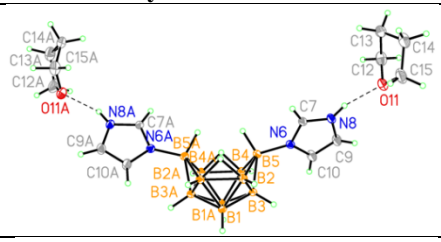	Not Measured
3, $(Him)B_{10}H_{12}$·Pyrazine	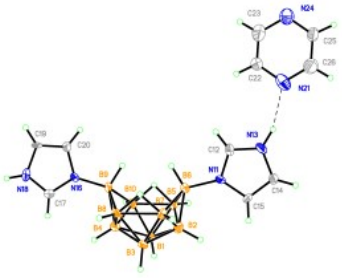	
4, $(Him)B_{10}H_{12}$·Nitrobenzene	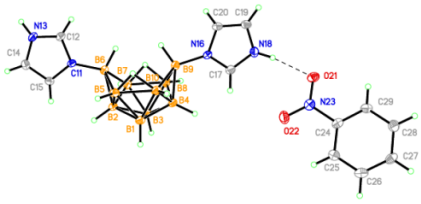	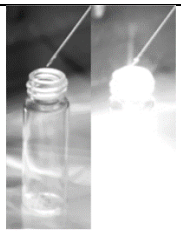
$(Toluidine)_2B_{10}H_{12}$·Toluidine·$C_6H_6$	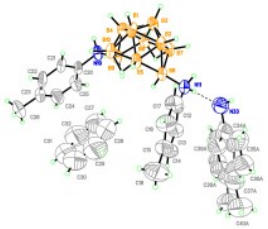	Not measured

References

(1) Ercolesi, F.; Adams, J. B. Interatomic Potentials from First-Principles Calculations: The Force-Matching Method. *EPL* **1994**.

3. Publications from this AFOSR funding

C. Carlin and M.S. Gordon, "Ab Initio Calculation of Anion Proton affinity and Ionization Potential: Sometimes less is more", J. Comp. Chem., 36, 597 (2015)

A. Findlater, F. Zahariev, and M.S. Gordon, "A Combined Fragment Molecular Orbital-Cluster in Molecule Approach to Massively Parallel Electron Correlation Calculations for Large Systems", J. Phys. Chem. A, 119, 3587 (**2015**)

C. Carlin and M.S. Gordon, "Ab Initio Investigation of Cation Proton Affinity and Proton Transfer Ability for Energetic Ionic Liquids", J. Phys. Chem A, 120, 6059 (**2016**)

T. Kudo, T. Taketsugu, and M.S. Gordon, "An Initio Molecular Dynamics Study of H_2 Formation Inside POSS Compounds. 2. The Effect of an Encapsulated Hydrogen Molecule", J. Phys. Chem A, 120, 8699 (**2016**)

K. Yanai, K. Ishimura, A. Nakayama, M.W. Schmidt, M.S. Gordon, and J. Hasegawa, "Electronic Polarization of the Water Environment in Charge-Separated Donor-Acceptor Systems: An Effective Fragment Potential Model System", J. Phys. Chem. A, 120, 10273 (**2016**)

Eliseo Marin-Rimoldi, Jindal K. Shah and Edward J. Maginn, "Monte Carlo simulations of water solubility in ionic liquids: A force field assessment", *Fluid Phase Equilibria*, **2016**, 407, 117-125.

Marta L. S. Batista, Helena Passos, Bruno J. M. Henriques, Edward J. Maginn, Simão P. Pinho, Mara G. Freire, José R. B. Gomes and João A. P. Coutinho, "Why are some cyano-based ionic liquids better glucose solvents than water?", *Physical Chemistry Chemical Physics*, **2016**, 18, 18958-18970.

Quintin R. Sheridan, Seungmin Oh, Oscar Morales-Collazo, Edward W. Castner, Joan F. Brennecke, and Edward J. Maginn, "Liquid Structure of CO_2-Reactive Aprotic Heterocyclic Anion Ionic Liquids from X-ray Scattering and Molecular Dynamics", *Journal of Physical Chemistry B*, **2016**, 120, 11951-11960.

Quintin R. Sheridan, William F. Schneider, and Edward J. Maginn, "Anion Dependent Dynamics and Water Solubility Explained by Hydrogen Bonding Interactions in Mixtures of Water and Aprotic Heterocyclic Anion Ionic Liquids", *Journal of Physical Chemistry B*, **2016**, 120, 12679-12686.

Jindal K. Shah, Eliseo Marin-Rimoldi, Ryan Gotchy Mullen, Brian P. Keene, Sandip Khan, Andrew S. Paluch, Neeraj Rai, Lucienne L. Romanielo, Thomas W. Rosch Brian Yoo, and Edward J. Maginn, "Cassandra: An Open Source Monte Carlo Package for Molecular Simulation", *Journal of Computational Chemistry*, **2017**, 38, 1727-1739.

Ryan Gotchy Mullen and Edward J. Maginn, "Reaction ensemble Monte Carlo simulation of xylene isomerization in bulk phases and under confinement", *Journal of Chemical Theory and Computation*, **2017**, 13, 4054-4062.

Mark B. Shiflett and Edward J. Maginn, "The Solubility of Gases in Ionic Liquids", *AIChE Journal*, invited "Perspectives" article, **2017**, 63, 4722-4737.

B.Q. Pham and M.S. Gordon, " Can Orbitals Really be Observed in STM Experiments?", J. Phys. Chem. A, 121, 4851 (**2017**)

M. W. Schmidt and M.S. Gordon, "The Effect of Boron Clusters on the Ignition Reaction of HNO_3 and Dicynanamide-based Ionic Liquids", J. Phys. Chem. A, 121, 8003 (**2017**).

Ryan Gotchy Mullen, Steven Corcelli and Edward J. Maginn, "Reaction Ensemble Monte Carlo Simulations of CO_2 Absorption in the Reactive Ionic Liquid Triethyl(octyl)phosphonium 2-Cyanopyrrolide", *Journal of Physical Chemistry Letters*, **2018,** 9, 5213-5218.

P. Xu, E.B. Guidez, C. Bertoni and M.S. Gordon, "Perspective: Ab Initio Force Field Methods Derived From Quantum Mechanics", J. Chem. Phys., 148, 090901 (**2018**).

S. Kim, C.M. Kaliszewski, E.B. Guidez and M.S. Gordon, "Benchmarking the Effective Fragment Potential Dispersion Correction on the S22 test set", J. Phys. Chem. A, in press.

B. Chan, J. Rintelman, G.P.F. Wood, L. Radom, and M.S. Gordon, "Solvation of the Glycyl Radical", J. Phys. Chem. A, in press. DOI: https://doi.org/10.1021/acs.jpca.8b06833

J. Conrad, S.R. Pruitt and M.S. Gordon, "Proton Transfer in 1,2,4-Triazolium Dinitramide: Effect of Microsolvation", J. Phys. Chem. A, in press. DOI: http://dx.doi.org/10.1021/acs.jpca.8b06348

4. Invited presentations from this AFOSR funding

"Intermolecular Interactions with Fragmentation Methods", Telluride Workshop on Intermolecular Interactions, Telluride, CO, July **2015**.

"Electronic Excited States: Solvent Effects and Dynamics", Pacific Basin Chemistry Conference, Honolulu, December **2015**.

"Intermolecular Interactions with Fragmengtation Methods", National American Chemical Society meeting, San Diego, March **2016**

"Predicting Nonlinear Optics with QM Methods", Materials Research Society meeting, March **2016**, Phoenix, AZ

"Unraveling the Structure and Dynamics of Electrolytes and Ionic Liquids via Molecular Simulation", Department of Chemical and Biomolecular Engineering seminar, University of Houston, Sept 30, **2016**.

"Will Molecular Modeling Ever Become a Mainstream Chemical Engineering Tool", AIChE annual meeting, San Francisco, CA, Nov. 16, **2016**.

"Molecular Dynamics Simulations of U_{20} Nanoclusters and Ligand Binding", Materials Science of Actinides workshop, University of Notre Dame, Nov. 21, **2016**.
"Intermolecular Interactions", Midwest American Chemical Society meeting, Oct. **2016**, Manhattan, KS

"Unraveling the Absorption Behavior and Structure of CO_2-Reactive Ionic Liquids via Molecular Simulation", Technical University of Delft Process Engineering and Energy Department colloquium, Delft, Netherlands, March 17, **2017**.

"Unraveling the Structure and Dynamics of Electrolytes and Ionic Liquids via Molecular Simulation", Department of Chemical, Biological and Materials Engineering colloquium, University of Oklahoma, Norman, OK April 19, **2017**.

"Cassandra: An Open Source Atomistic Monte Carlo Package for Materials Simulation", Scimeeting Europe: Materials Modeling and Simulation Conference, Athens, Greece, June 22, **2017**.

"Dispersion in Intermolecular Interactions", 11th Triennial Congress of the World Association of Theoretical and Computational Chemists, Munich, Germany, August **2017**.

"Energetic Ionic Liquids and Endothermic Fuels", AFOSR Molecular Dynamics meeting, Albuquerque, NM, May **2018**

"Computational Design of New Materials for Energy Efficient Separations", Department of Chemical and Petroleum Engineering colloquium, University of Pittsburgh, Pittsburgh, PA, Jan. 26, **2018**.

"Intermolecular interactions Using Fragmentation Methods", Telluride Meeting on QM/MM Methods in Excited States and Photochemistry, Telluride CO, July **2018**

"Structure and Dynamics of Ionic Liquids from Atomistic Simulations", Department of Chemistry, Physical Chemistry Seminar, University of Rome Sapienza, Rome, Italy, March 14, **2018**.

"Computational Design of New Materials for Energy Efficient Separations", Department of Chemical and Environmental Engineering colloquium, University of California at Riverside, Riverside, CA, April 6, **2018**.

"Computational Design of New Materials for Energy Efficient Separations", Department of Chemical and Petroleum Engineering colloquium, University of Kansas, Lawrence, KS, April 10, **2018**.

5. Contributed presentations from this AFOSR funding

Ryan Gotchy Mullen, Steven Corcelli and Edward J. Maginn, "Molecular Simulation of CO2 Absorption in the Ionic Liquid [P2228][2-Cnpyr] Using Reaction Ensemble Monte Carlo", AIChE Annual Meeting, San Francisco, CA, Nov. 14, **2016**.

Eliseo Marin-Rimoldi and Edward J. Maginn, "Recent Advances in the Development of Cassandra: An Open Source Monte Carlo Framework for Phase Equilibria Calculations", AIChE Annual Meeting, San Francisco, CA, Nov. 14, **2016**.

Ryan Gotchy Mullen and Edward J. Maginn, "Reaction Ensemble Monte Carlo Simulations of Xylene Isomerization Under Confinement", AIChE Annual Meeting, Minneapolis, MN, Oct. 31, **2017**.